Drying Effects of Cross-Flow Air Circulation On Wheat Stored in Deep Cylindrical Bins

by
D. L. Day and
G. L. Nelson

Technical Bulletin, No. T-106
January 1964

CONTENTS

Drying Effect of Cross-Flow Air Circulation on Wheat Stored in Deep Cylindrical Bins

by

D. L. Day and G. L. Nelson*

Cross-flow air systems seem potentially suitable for drying grain stored in tall, upright cylindrical bins because the shorter air circulation path reduces air resistance to reasonable values. As a result, smaller motors and blowers can be used in a cross-flow system, and the capital and operating costs are reduced. During prolonged storage, cross-flow systems can be used with reduced air circulation for grain cooling and fumigation.

This bulletin reports results of a study made to determine the drying effect of cross-flow air systems on wheat stored in deep cylindrical bins. Equations were developed to predict the drying effect over a range of grain and air conditions.

Figure 1 shows a schematic drawing of a vertical air flow system and a cross-flow system, typical of those used in Oklahoma and other Southwest grain areas.

Duct Arrangements

Figure 2 shows three cross-flow arrangements, differing in number and positions of inlet and exhaust ducts, which were studied. The two-duct system requires less duct-work, but air circulation power requirements were expected to be higher than for the four- and six-duct systems. Uniform moisture distribution throughout the bin contents after completion of drying is desirable. The degree of uniformity during the drying process was thought to depend on the number of ducts.

In all experiments, the air circulation paths were as shown. The air circulation paths for the four- and six-duct arrangements can be modified by different choices of ducts to use for inlets and exhausts, but choices other than shown in Figure 2 were not investigated.

Research reported herein was done under Oklahoma Station project 679.

* Former graduate assistant now Assistant Professor, Agricultural Engineering department, University of Illinois; and Professor, Agricultural Engineering department, Oklahoma State University.

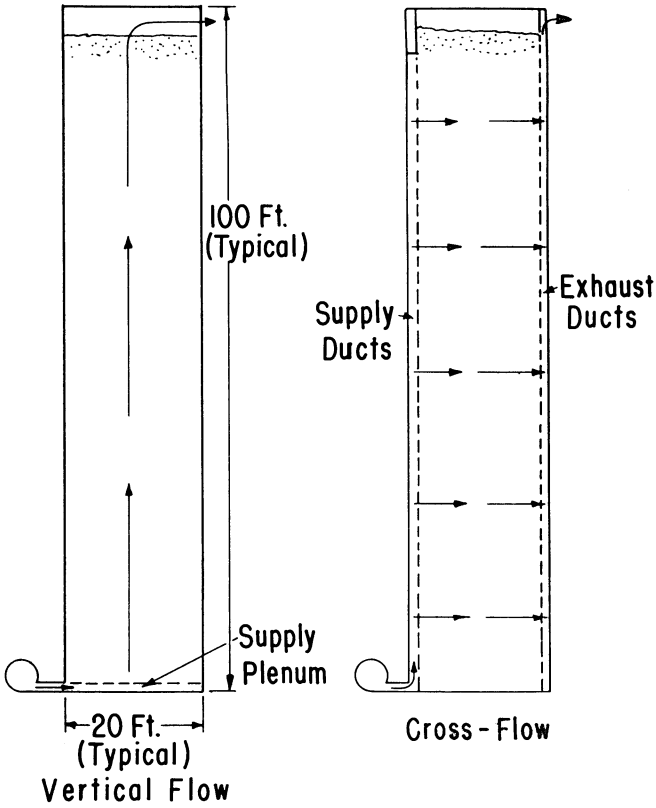

Figure 1. Typical configurations of vertical flow and cross-flow drying systems in deep cylindrical storages

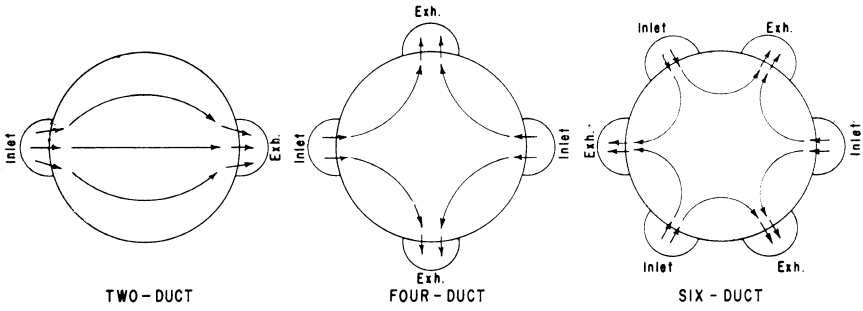

Figure 2. Cross-flow duct arrangements

Experiment Design

Dimensional analysis and similitude were employed in designing the experiments. The pertinent quantities are listed in Table 1. Items 3 and 5 in Table 1 are defined graphically in Figures 3 and 4, respectively. From these quantities, dimensionless parameters were formed and used in subsequent analyses. These parameters are listed in Table 2. The general relationship to define by analysis of the experimental results is:

eq (1)

$$\Pi_1 = F(\Pi_2, \Pi_3, \cdots, \Pi_{11})$$

The parameter Π_1 is regarded as dependent. The others may be regarded as independent parameters. The experimental method consisted of varying the value of each independent parameter, one at a time, through a pre-determined range of values while holding the values of the other independent parameters constant. The dependent parameter was thus measured as a function of the independent parameter undergoing variation. The independent parameters were controlled in laboratory experiments by grain initial moisture content and temperature; air temperature, moisture content, and circulation rate entering the grain; initial bin temperature; and air temperature between the insulated bin lining and the outer jacket.

This method produced component equations, each of which related the dependent parameter to only one independent parameter. The component equations were then combined by mathematical analysis to establish a general prediction equation relating the dependent parameter to all the independent parameters.

Equipment and Procedures

Three sizes of bins were used: 5-7/8 in., 2 ft. 0 in., and 4 ft. 8 in. diameters. The larger bins were used to validate the prediction equation formulated from data obtained with the 5-7/8 in. diameter bins. These latter bins were tested in an indoor laboratory where conditions were carefully controlled. The 2 ft. 0 in. and 4 ft. 8 in. bins were tested in outdoor sheds using ambient air. Each of the three cross-flow duct arrangements shown in Figure 2 was tested in the 5-7/8 in. and 2 ft. bins; but only the two-duct arrangement was tested in the 4 ft. 8 in. diameter bin.

Table 1 Pertinent quantities for drying effect in cross-flow systems

No.	Quantity	Description	Dimension*
1.	M_R	Average moisture removed from grain, % dry basis.	——
2.	t	Elapsed time of dryer operation, min..	T
3.	ΔM	Difference, $(M_g)_i - M_e$, lbs. moisture per lb. of dry grain; dry basis, as a decimal. $(M_g)_i$ = Initial grain moisture content, dry basis as a decimal. M_e = Grain moisture content in equilibrium with air entering grain, dry basis as a decimal. (Cf. figure 3)	——
4.	τ_e	Air dry bulb temp. entering grain, F abs.	θ
5.	$\Delta\tau$	Difference, $\tau_e - \tau_l$, F τ_l = Ideal temp. of air leaving grain, F abs. (Cf. figure 4)	θ
6.	τ_g	Initial grain temp., F abs.	θ
7.	ρ_g	Bulk density of grain, lb_m/ft^3.	ML^{-3}
8.	c_g	Grain specific heat, Btu/(lb_m-deg. F)	$HM^{-1}\theta^{-1}$
9.	k_g	Grain thermal conductivity, Btu/ft-deg. F-Min.	$HL^{-1}T^{-1}\theta^{-1}$
10.	$\Delta\tau_w$	Difference, $\tau_e - \tau_o$, F. τ_o = Dry bulb temp. of ambient air around bin, F abs.	θ
11.	Q_a	Total air circulation rate through bin, (ft^3 of air/min.)/ft^3 grain.	T^{-1}
12.	ρ_a	Density of air entering grain, lb_m/ft^3	ML^{-3}
13.	c_a	Specific heat of air entering bin, Btu/(lb_m-deg. F)	$HM^{-1}\theta^{-1}$
14.	U	Bin wall overall heat transmission coef., Btu/min.-ft^2-deg. F.	$HT^{-1}L^{-2}\theta^{-1}$
15.	r	Hydraulic radius of cylindrical bin, ft.	L
16.	S	Circumferential spacing of vertical cross-flow ducts, bin circumference/no. of ducts, ft.	L

* Note: Dimensional Symbols are.
L - Length, M - Mass, H - Heat, θ - Temperature, T - Time

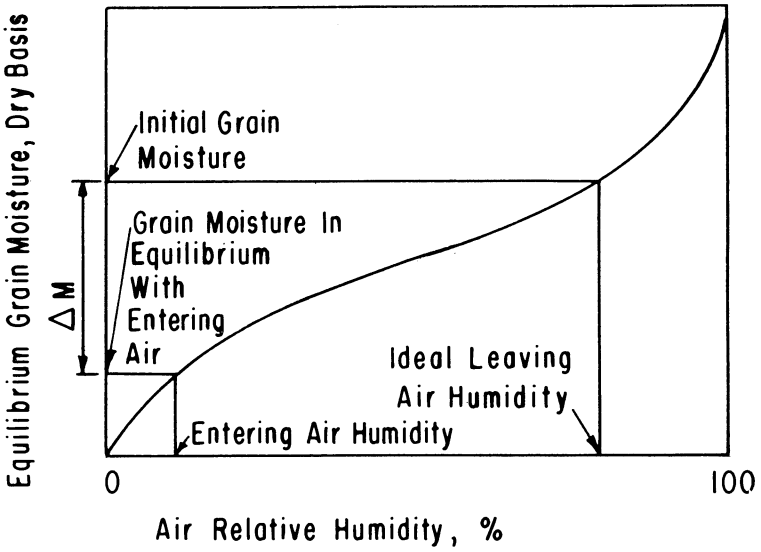

Figure 3. Desorption isotherm for computation of △ M

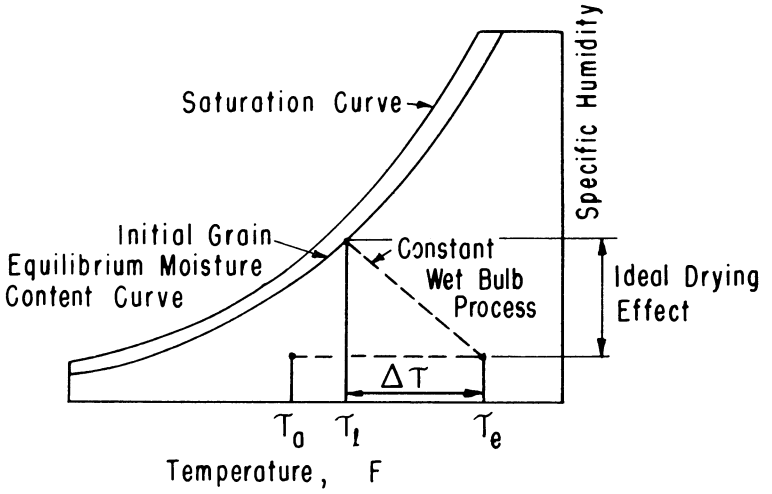

Figure 4. Skeleton psychrometric chart to illustrate computations of $\Delta\tau$

Table 2 Dimensionless parameters for analysis of cross-flow drying effect

$\pi_1 = M_R$	Drying effect
$\pi_2 = \Delta M$	Drying potential for grain
$\pi_3 = \Delta T / T_e$	Heating potential from air
$\pi_4 = C_g \rho_g r^2 / k_g t$	Thermal diffusivity index
$\pi_5 = T_e / T_g$	Air - grain temperature ratio
$\pi_6 = Q_a t$	Air circulation index
$\pi_7 = U / \rho_a C_a Q_a r$	Index of ratio of heat transfer per unit temperature drop across wall to available sensible heat from air per unit temperature change of circulating air
$\pi_8 = \Delta T_w / T_e$	Ratio of temperature drop across wall to temperature of entering air
$\pi_9 = \rho_g / \rho_a$	Grain / air density ratio
$\pi_{10} = C_g / C_a$	Grain / air sp. ht. ratio
$\pi_{11} = r / S$	Duct spacing index

The 5⅞ in. model bins were built from plastic tubing as shown in Figure 5. The equipment used in the laboratory is illustrated in Figures 6 and 7. A small blower, at the left end of the plenum chamber, was used to supply air. The plenum chamber was an insulated, rectangular box with internal electrical strip heaters. The model bins were lined outside with insulation and surrounded by an insulated chamber, Figure 7. The model bin and its contents were hung from a scale for weighing the bin and its contents in place at intervals without removing it from the insulated chamber. The weight loss corresponded to change in moisture content. Static pressure in the plenum chamber was measured with a precision manometer.

The 2 ft. diameter bins were built from galvanized sheet steel as shown in Figure 8. They are shown at the test installation in Figure 9. Grain moisture content was determined by sampling the bins with a miniature grain trier. Air flow rate was measured with a pitot-static tube in the blower duct. Temperatures and pressures inside the bin were measured with sensing elements on probes.

The 4 ft. 8 in. diameter, two-duct bin was built from a salvaged steel tank as shown in Figure 10. Figure 11 shows the outdoor test site. Instrumentation for this bin was similar to that for the 2 ft. diameter bins.

Wheat used in the 5⅞ in. diameter and 2 ft. 0 in. diameter bins was Kaw variety from the 1961 harvest in the Stillwater area. It had a test weight of 61.5 lbs/bu; 0.10 percent foreign matter, 0.90 percent damaged kernels, 0.80 percent dockage. Except for the high moisture content (14.6 percent, wet basis) it met grade requirements for No. 1 wheat.

Wheat used for the experiments in the two-duct, 4 ft. 8 in. diameter bin experiments was Comanche variety from the 1962 harvest in the Stillwater area. It was uncleaned and had a moisture content of 21.3 percent, dry basis.

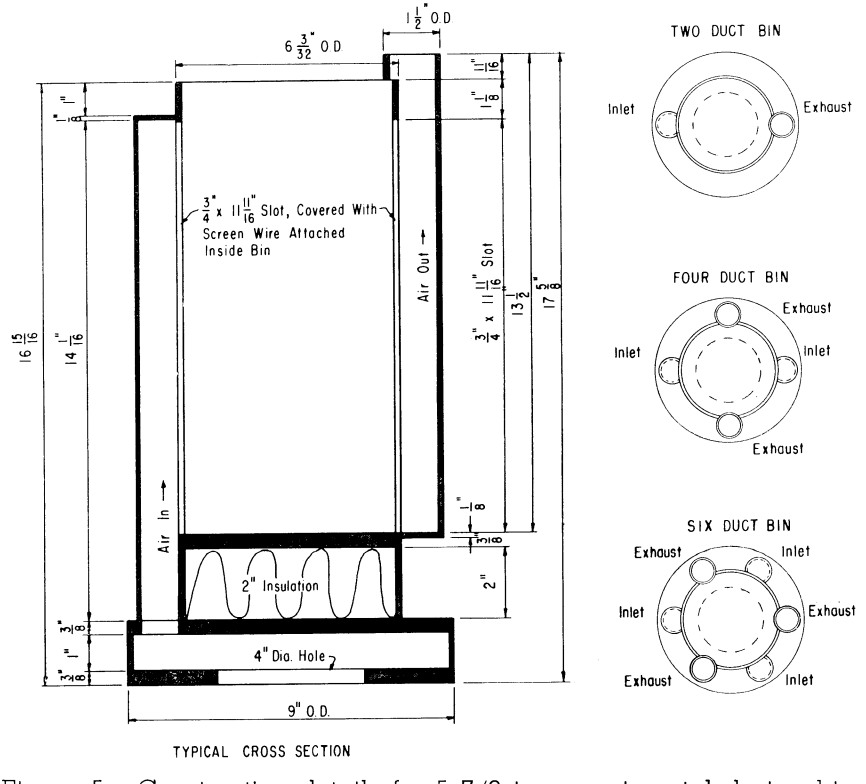

Figure 5. Construction details for 5 7/8 in. experimental drying bins

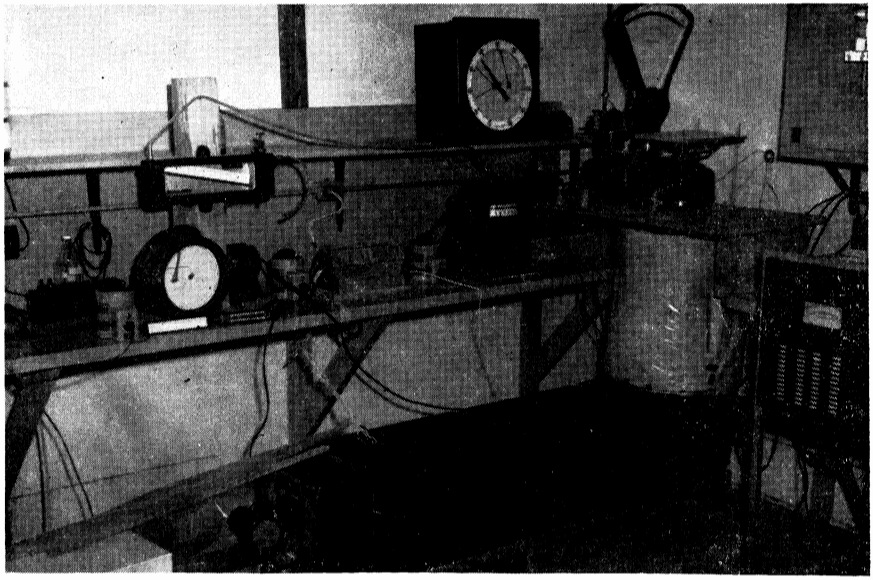

Figure 6. Auxiliary equipment for 5 7/8 in. experimental bins

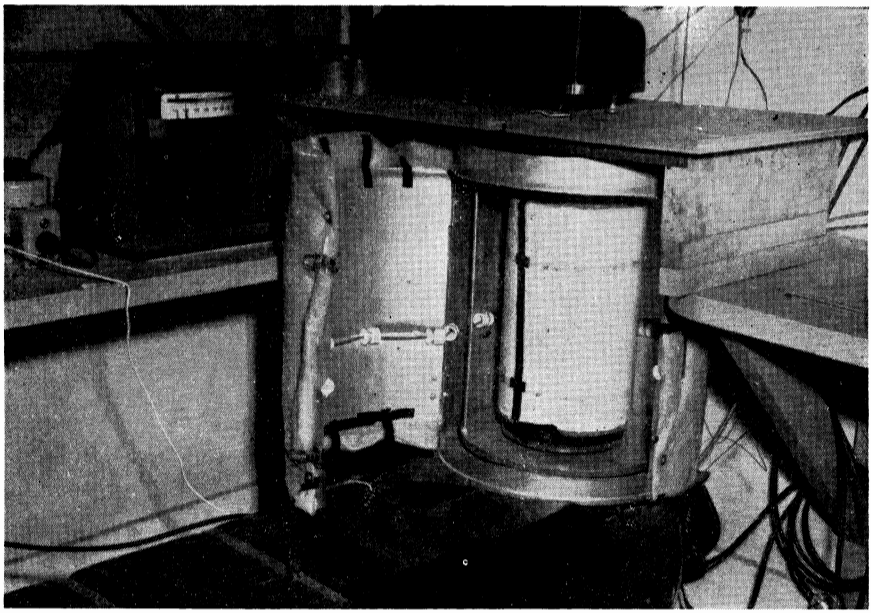

Figure 7. Outer insulated housing and insulating Jacket for 5 7/8 in. bins

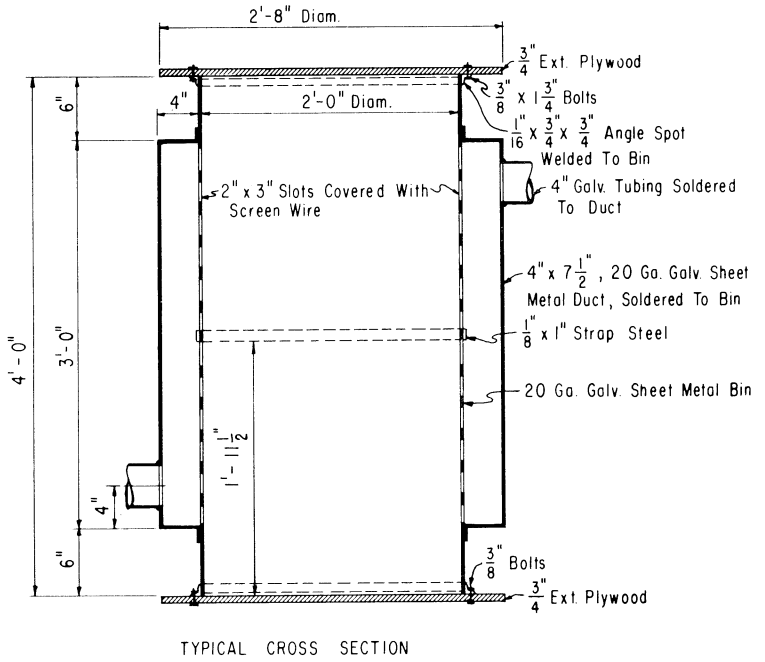

Figure 8. Construction details, 2 ft. bins

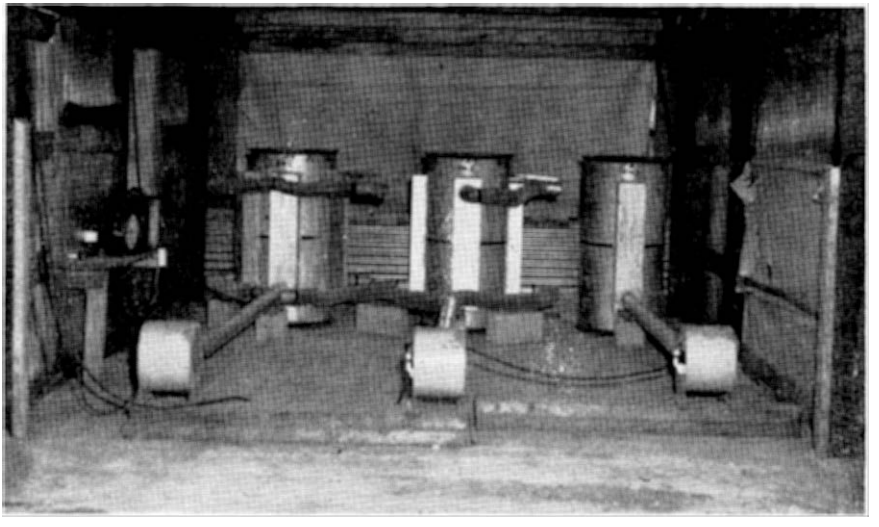

Figure 9. Outdoor test shelter and installation, 2 ft. bins

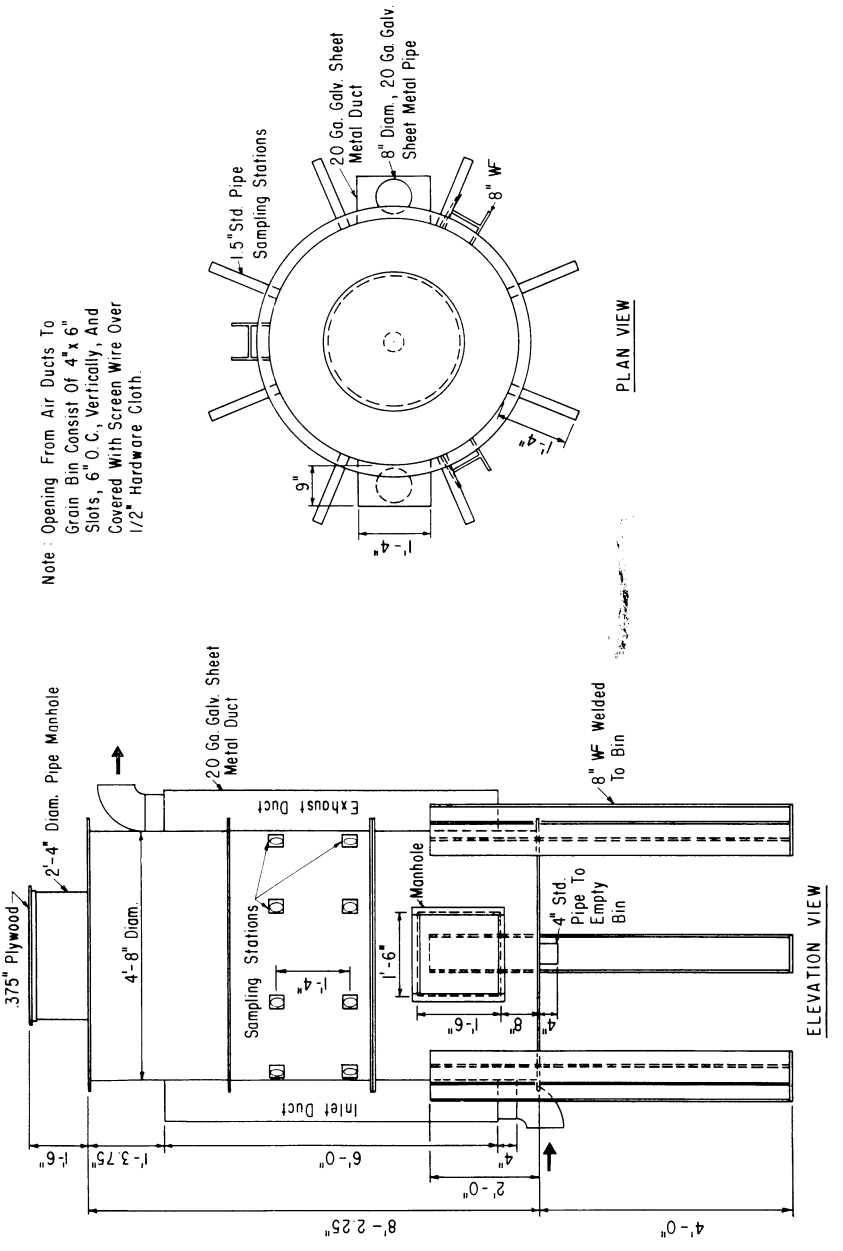

Figure 10. Construction details, 4 ft. 8 in. bins

Figure 11. 4 ft. 8 in. bins installed at test site

Results

Analysis of the component equations, as described in detail by Day [1], showed that an appropriate form of the general equation was:

eq. (2)

$$\Pi_1 = \left[f_1(\Pi_2, \Pi_3)\right] \times \left[1 - e^{f_2(\pi_2, \pi_3, \cdots, \pi_6)}\right]$$

Parameters Π_7, Π_8, Π_9 and Π_{10} do not appear in eq. 2. Preliminary analysis of the data obtained during experiments to measure the effect of Π_7 and Π_8 revealed that system performance was virtually unaffected

by changes in these parameters, which are indices of heat transfer through the bin walls in relation to sensible heat in the circulating air. As a result of this analysis, the effects of Π_7 and Π_8 were ignored in subsequent analysis, and these parameters were omitted from equation (2).

Parameter Π_9, the grain-air density ratio was not accounted for in the experiment design, data analysis, or prediction equation because of the virtual impossibility of varying it over an appreciable range while controlling other parameters which are influenced by air temperature. It is presumed that under prototype operation conditions, variations in Π_9 are small enough to be neglected. Parameter Π_{10} is virtually constant for a given grain.

Parameter Π_{11}, the duct spacing index, was not explicitly accounted for in prediction equation (2). Instead, the coefficients and exponents were evaluated separately as shown in Table 3 for each bin type. Each bin type corresponds to a different but constant value of Π_{11}.

Table 3—Numerical values for coefficients and exponents in equations 3 and 4.

	Two duct	Four duct	Six duct
C_1	91.314	91.314	91.314
C_2	0.40531	0.40531	0.40531
C_3	0.00012613	0.00011896	0.00011555
C_4	0.19521	0.23117	0.30529
C_5	2.2254	2.2369	2.0147
C_6	22,569.	22,658.	21,320.
C_7	—965,243.	—1,051,880.	—805,346.

The functions f_1 and f_2 were found to be defined by:

eq. (3)

$$f_1(\Pi_2, \Pi_3) = C_1(\Pi_2 \times \Pi_3)^{C_2}$$

and

eq. (4)

$$f_2(\Pi_2, \Pi_3, \cdots, \Pi_6) = C_3 \Pi_4^{C_4} \Pi_5^{C_5} \left[(\Pi_5 - 1)(C_6 + C_7 \Pi_2 \Pi_3) - \Pi_6\right]$$

The coefficients C_1 and C_2 were evaluated by using wheat desorption isotherm data and the condition that the maximum attainable value of Π_1 is:

eq. (5)

$$\Pi_{1(MAX.)} = C_1(\Pi_2 \times \Pi_3)^{C_2}$$

The coefficients C_3 and C_4 were evaluated by simultaneous solutions of component equations obtained by least squares regression analysis.

The coefficients C_5, C_6 and C_7 were evaluated by an iterative least squares analysis. The values established for the coefficients C_1, C_2, ... C_7 are given in Table III. These are refined values based on additional analyses completed after the original study by Day (ref. 1).

Discussion

Equation (2) is applicable for predicting drying effect when $\Pi_5 \geqq 1$. For $\Pi_5 < 1$, equation (2) is applicable only after sufficient operating time, "t", has elapsed to satisfy the following equation:

eq. (6)

$$\pi_6 \geqq |(\pi_5 - 1)(C_6 + C_7 \pi_2 \pi_3)|$$

This limitation is illustrated in Figure 12.

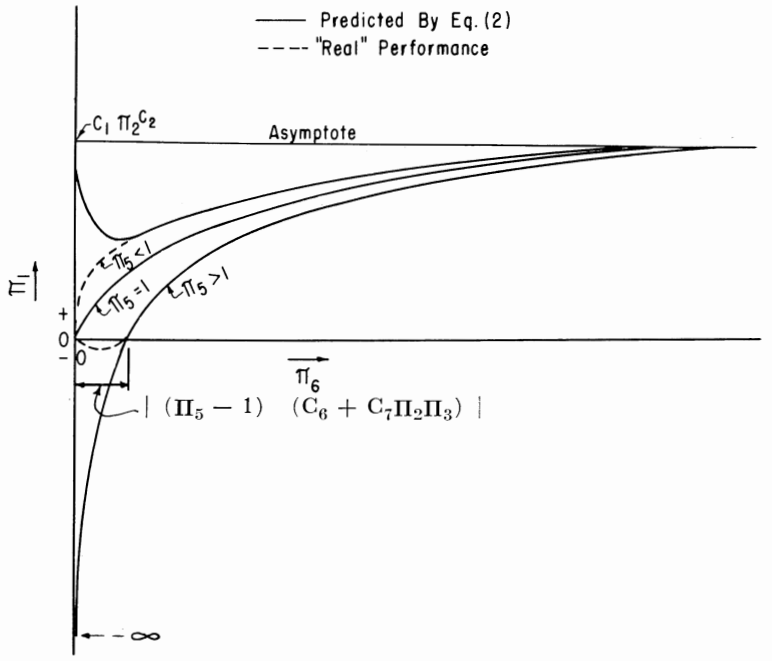

Figure 12. Lower limit of π_6 for applicability of prediction eq. (2)

Validity of the prediction equations is shown by the plots of predicted Π_1 versus observed Π_1, in Figure 13, 14, and 15 for the duct arrangements and sizes of bins investigated.

Equation (2) predicts *average moisture* reduction of the bin contents. It does not indicate moisture variation in the direction of air flow through bin contents. The zones which dry last and therefore are highest in moisture at termination of drying for each bin type are illustrated in Figure 16. These are qualitative indications. The quantitative variation in grain moisture during and after drying depends on initial and operating conditions. If drying is prolonged, all of the bin contents will come eventually into close equilibrium with the entering air.

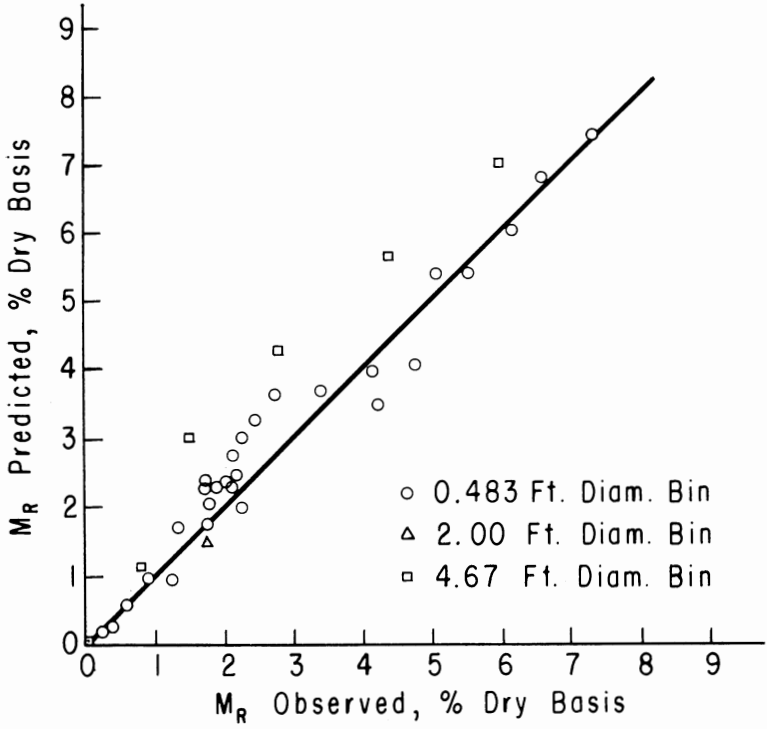

Figure 13. Predicted drying effect by eq. (2) compared to observed drying effect for two-duct system

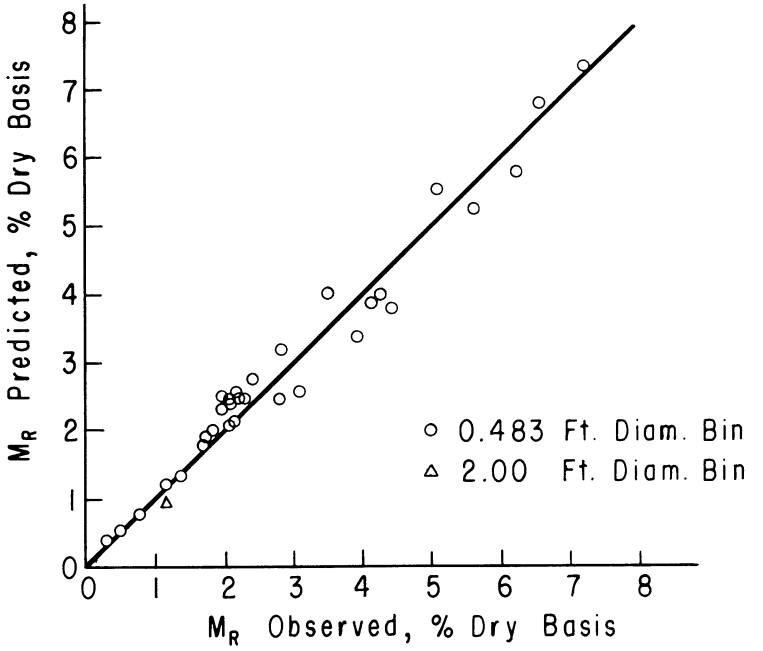

Figure 14. Predicted compared with observed drying effect for four-duct bin

Equation (2) was developed from data for steady-state operating conditions that prevailed for the small models in the laboratory. The larger models tested outdoors were operated in naturally varying, largely uncontrolled air conditions. To apply the equation to these conditions, operating time - averaged values of air temperature and humidity were used. Drying effect is a non-linear function of air temperature, humidity and time. As a result, some loss in prediction precision occurred when time-averaged values of temperature and humidity were used to predict drying effect with naturally varying air conditions. This loss in precision is readily apparent for the points plotted in Figure 13 for the 4 ft. 8 in. diameter bin.

In the two-duct arrangement, only one air circulation path exists. In the four or six-duct arrangements, two or three paths exist. It is hypothesized that the additional paths minimized the effect of isolated pockets of grain initially at a different condition than the otherwise uniform bin contents. These pockets if near the inlet or exhaust duct of the two-duct bin could temporarily produce a drying effect differing appreci-

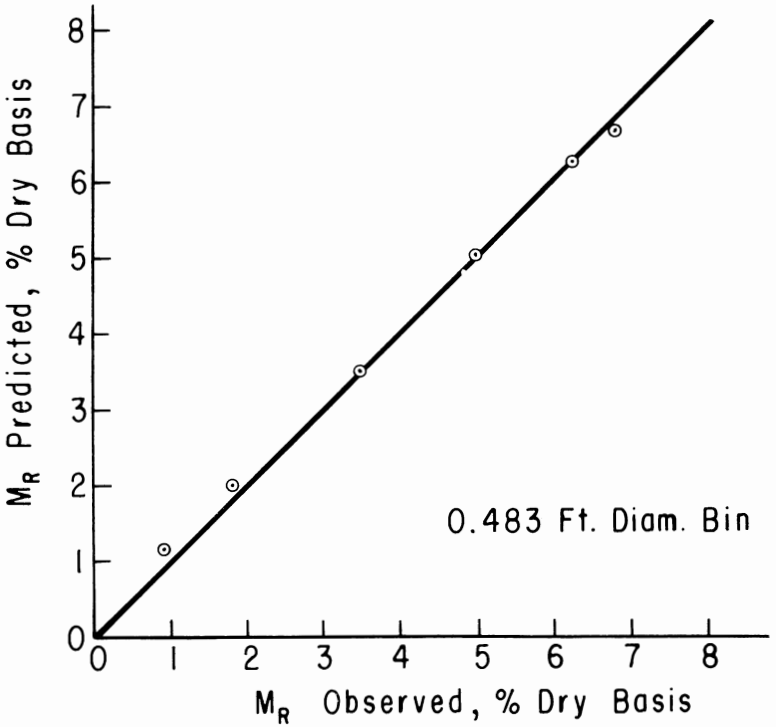

Figure 15. Predicted compared with observed drying effect for six-duct bin

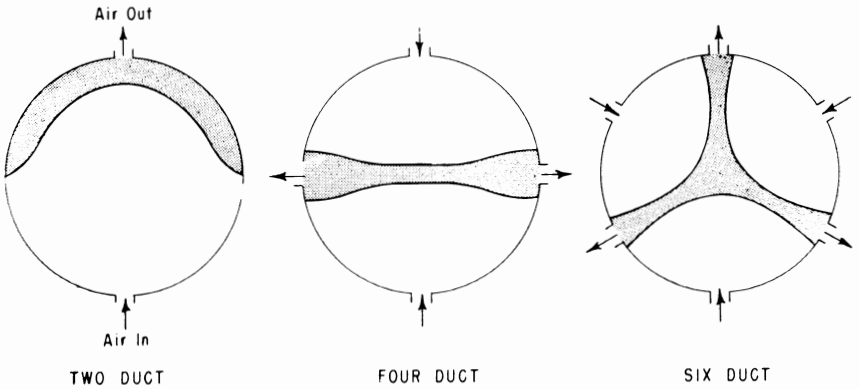

Figure 16. Effect of duct arrangement on generalized drying pattern in cross-flow systems. Shaded zones are last to dry

ably from that predicted according to uniform initial conditions. This hypothesis is supported by the standard errors of estimate for predicted drying effect, M_R, which were:

Six-duct arrangement	0.19
Four-duct arrangement	0.34
Two-duct arrangement	0.41

Prediction equation (2) relates moisture removed to an air circulation index. This index is the product of elapsed time and air circulation rate. If air circulation is prolonged indefinitely, the amount of moisture removed approaches closely a limiting value determined only by $C_1(\Pi_2 \times \Pi_3)^{C_2}$

The prediction equation does not lend itself to desk calculator analysis of specific cross-flow systems. Analyses developed with high-speed computer programs can be presented in tabular or graphic form. Examples of such analyses based on high speed computer solutions of equation (2) for the two-duct configuration are given in Figures 17, 18, and 19.

Figure 17 illustrates the effect of $(\Delta M \times \Delta\tau/\tau_e)$ on the maximum attainable drying effect, even with prolonged operation. Figure 18 shows the effect of bin diameter on drying. Although larger bin diameters produce faster drying for the same value of $Q_a \times t$, the drying effect in each bin size approaches the same asymptotic value as determined by $(\Delta M \times \Delta\tau/\tau_e)$.

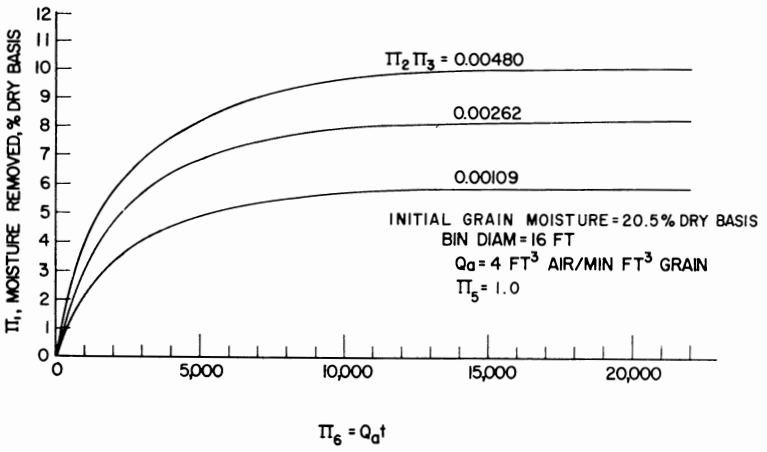

Figure 17. Typical effect of variation in product, π_2 π_3 on drying rate

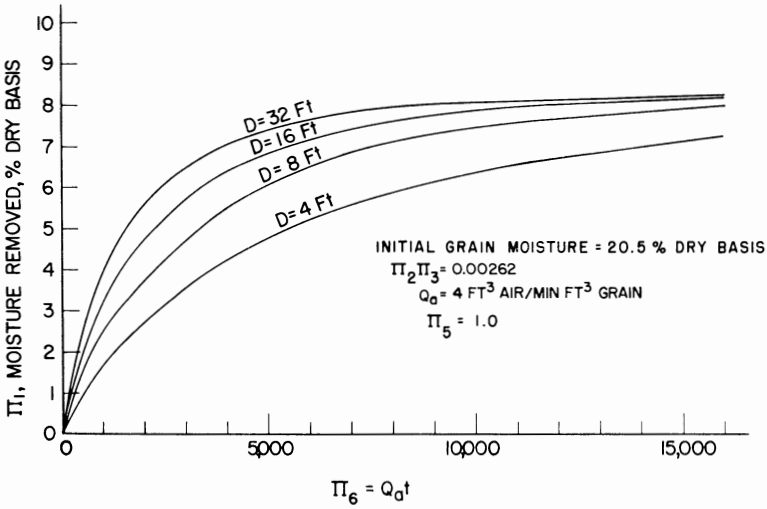

Figure 18. Typical effect of bin diameter on drying rate

Variations in drying effect due to changes in Q_a, air flow rate, are predictable from eq. (2). Since drying time, t, appears in Π_4 and Π_6, the drying effect, M_R, IS NOT the same for equal values of Π_6 obtained by different combinations of values of Q_a and t. For example, doubling the air flow rate and reducing elapsed time by one-half results in an increased drying effect for the doubled air flow rate as shown by the typical analyses graphed in Figure 19. This effect is attributable to improved heat and mass transfer coefficients for the kernel-air interface.

It is apparent from inspection of Figure 12 that variations in the parameter τ_e/τ_g have an important influence on drying effect. When the entering air is initially warmer than the grain, $\tau_e/\tau_g > 1.0$. An initial "warmup" period elapses during which a small negative drying effect can occur. This is illustrated in Figures 12 and 20. As operation continues, the grain temperature is raised sufficiently to start producing a positive drying effect which increases asymptotically to a limit. When the grain is initially warmer than entering air, sensible heat is transferred from the grain to the air. This increases the drying effect for a specified air temperature, compared to the drying effect obtained when $\Pi_5 \leqq 1.0$.

Equation (2) is applicable only for values of Π_6 specified by equation (6). However, this limitation applies only in the earliest part of a typical drying operation and does not restrict application of the equation to practical situations.

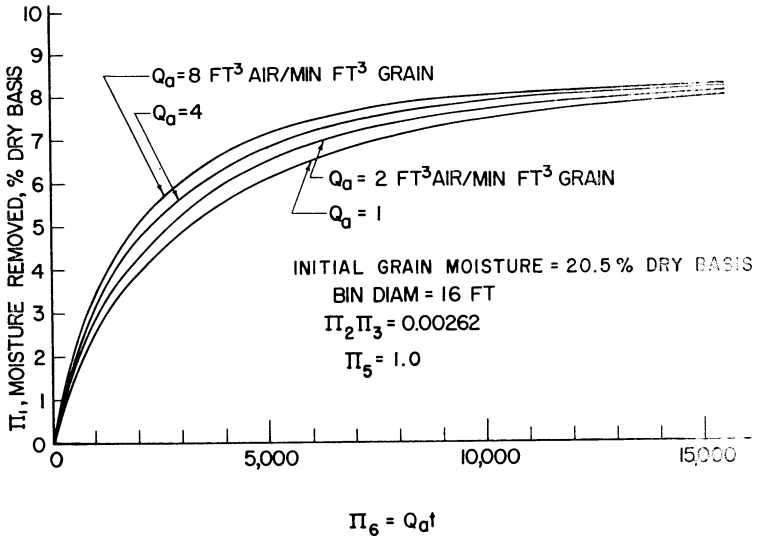

Figure 19. Typical effect of air circulation rate on drying rate

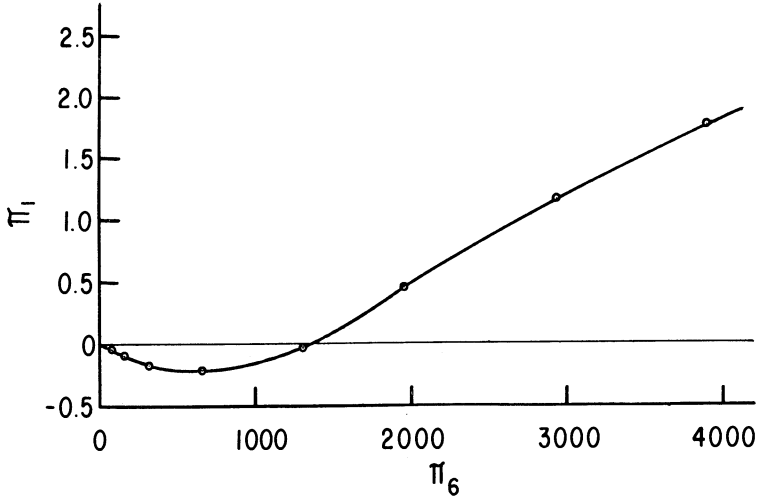

Figure 20. Typical drying system performance when $\pi_5 > 1.0$

Drying rates computed by equation (2) with the coefficients in Table 3 revealed that drying rate is virtually the same for all three duct arrangements studied. A comparison for a two-duct and four-duct bin is shown in Figure 21.

Table IV lists the range of experimental values of the dependent and independent parameters encompassed by the experiments with the 5⅞ in. and the 2 ft. diameter bins. Equation (2) can be expected to be valid for estimating drying effect for prototype bins within the range of values listed on Table IV.

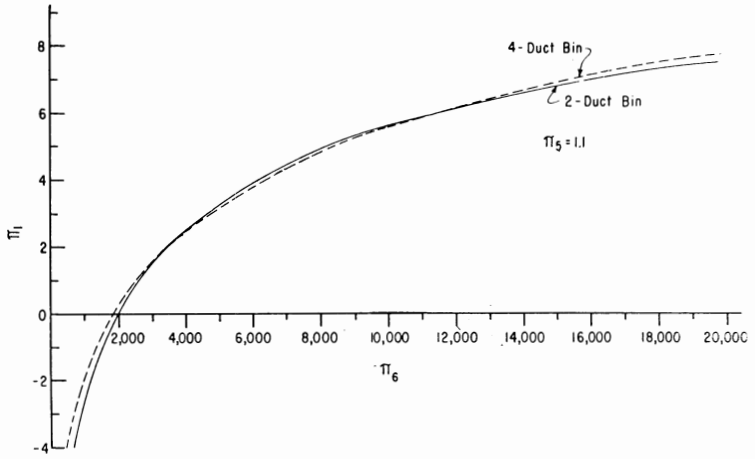

Figure 21. Typical comparison of predicted drying effect for two-duct and four-duct systems

Table 4 Range of values for dimensionless parameters encompossed by experiments with 5 7/8 in. and 2 ft. diameter bins

PARAMETER	RANGE
M_R	-0.83 to +7.34
$\Delta M \times \frac{\Delta \tau}{\tau_e}$	0.00403 to 0.0195
$c_g \rho_g r^2 / k_g t$	0.88 to 42
τ_e / τ_g	0.966 to 1.141
$Q_0 t$	0 to 20,000

Summary and Conclusions

An analytical investigation based on experimental results from models and prototype of cross-flow grain drying systems was conducted to obtain prediction equation (2) p. 13, which defines system performance. It can be used to predict wheat drying rates and final moisture contents as a function of system design and operating variables listed in Table 1.

Scaled-down drying system models can be used to analyze the performance of prototype grain drying systems and to obtain quantitative prediction equations.

Drying rate and maximum drying effect obtainable can be defined by a prediction equation of the form of eq. (2) which accounts for entering air temperature, humidity, and circulation rate; elapsed time of operation; grain initial temperature; grain initial moisture content; and bin diameter.

Drying rate and maximum drying effect are virtually unaffected by variations in the overall thermal conductance of the bin wall. No significant improvement in drying rate can be expected from insulating the walls.

The same drying rate based on average moisture reduction occurs in all three duct configurations studied. However, the pattern of moisture distribution across the bin between inlet and outlet ducts varied radically among the three duct configurations.

References

(1) Day, Donald Lee. Experimental analysis of cross-flow grain drying systems in deep cylindrical bins. Ph.D. Thesis. Library, Oklahoma State University. 1962.

(2) Day, D. L., G. L. Nelson, and G. Burns Welch. Analysis of static pressures for cross-flow air circulation in deep cylindrical bins. OAES bulletin in preparation.

(3) Granet, William and Clark Edwards. IBM-650 programs for general linear and non-linear regression calculations. Stillwater, Oklahoma. O.S.U. Computing Center and Department of Agricultural Economics. (Mimeographed)

Oklahoma's Wealth in Agriculture

Agriculture is Oklahoma's number one industry. It has more capital invested and employs more people than any other industry in the state. Farms and ranches alone represent a capital investment of four billion dollars—three billion in land and buildings, one-half billion in machinery and one-half billion in livestock.

Farm income currently amounts to more than $700,000,000 annually. The value added by manufacture of farm products adds another $130,000,000 annually.

Some 175,000 Oklahomans manage and operate its nearly 100,000 farms and ranches. Another 14,000 workers are required to keep farmers supplied with production items. Approximately 300,000 full-time employees are engaged by the firms that market and process Oklahoma farm products.

1-64/2M